Elastic and inelastic mean-free-path determination in solid xenon from electron transmission experiments

G. Bader*
Département de Physique et Groupe de Recherche sur les Semiconducteurs et les Diélectriques, Faculté des Sciences, Université de Sherbrooke, Sherbrooke, Québec J1K 2R1, Canada

G. Perluzzo
Groupe CRM en Sciences des Radiations, Département de Médecine Nucléaire et de Radiobiologie, Faculté de Médecine, Université de Sherbrooke, Sherbrooke, Québec J1K 2R1, Canada

L. G. Caron
Département de Physique et Groupe de Recherche sur les Semiconducteurs et les Diélectriques, Faculté des Sciences, Université de Sherbrooke, Sherbrooke, Québec J1K 2R1, Canada

L. Sanche
Groupe CRM en Sciences des Radiations, Département de Médecine Nucléaire et de Radiobiologie, Faculté de Médecine, Université de Sherbrooke, Sherbrooke, Québec J1K 2R1, Canada

(Received 6 April 1982)

Electron transmission experiments in the (0—20)-eV energy range have been performed on Xe films (0—3000 Å) deposited at various temperatures on different metal substrates [Nb,Pt,W(100)]. A theoretical model is used to extract from these experiments the elastic and inelastic mean free paths in the (0—8.5)-eV energy region. Some structures in the transmitted current arise from inelastic processes and yield information on electronic excitations (excitons and electron-hole—pair creation) and the energy of the bottom of the conduction band. Other structures present in the elastic mean free path appear to be caused by structural effects and thermal disorder of the deposited film.

I. INTRODUCTION

Low-energy (0—20 eV) electron attenuation lengths or mean free paths (MFP's) in semiconductors and insulators have been measured in the past by photoelectron transmission techniques.[1—9] In a typical experiment, the photoexcited electrons escape from the solid into vacuum. The total yield and the energy distribution of the photoexcited electrons are measured as a function of the film thickness and photon energy. Electron attenuation lengths are deduced from these data. The measured signal depends on a number of parameters (e.g., optical absorption cross sections and optical reflectance) which are not related to the electron scattering mechanism. Furthermore, any determination of the energy dependence of MFP requires deconvolution procedures which are often not unique.

In this paper, we show that it is possible to determine the energy dependence of absolute elastic and inelastic MFP in insulators and semiconductors from a simple electron transmission experiment.[10] The method consists of directing a well-collimated monochromatic electron beam of variable energy to a metal substrate and measuring the attenuation of the beam as a function of the thickness of a film grown on the substrate. The range of applicability of quantitative MFP determination extends from the vacuum energy level up to energies above the first electronic excitation threshold. *A priori,* there are no restrictions on the nature of the film as long as it does not charge too rapidly. In addition to MFP measurements, the transmission spectra reveal a number of interesting features related to the order of the film, the position of the bottom of the conduction band, the threshold excitation function for the lowest-energy exciton, and the photoelectric threshold.

Knowledge of low-energy elastic and inelastic MFP is important in interpreting photoemission[11] and low-energy electron diffraction[12] (LEED) data since these parameters determine the probing depth. Electron MFP's are also needed to achieve a better understanding of electron interactions with dielectric solids. These interactions are fundamental to those mechanisms associated with radiation effects in organic and biological materials.

We have chosen first to apply our method to xenon films for the following reasons. A number of parameters, including the electron affinity, the band gap, and the photoelectric threshold, are already well known for this solid.[13,14] Xenon can be condensed at relatively high temperatures allowing a suitable range of temperature variation. The crystalline structure of Xe multilayers films on Ir(100) and Nb(100) has been investigated by LEED[15] and electron energy-loss spectroscopy,[16] respectively. Finally, only acoustic phonons exist in solid Xe.[17] These are expected to contribute only slightly to the dissipation of the electron energy due to the small electron-phonon coupling constant[8] and short time spent by electrons in the film. Thus, the energy range 0—8 eV provides a wide region where elastic scattering can be studied with negligible interference from inelastic events.

The experiment is described in Sec. II. In Sec. III, transmission spectra are reported for Xe films of different thicknesses and temperatures deposited on Nb, Pt, and W(100) substrates. Section IV describes a phenomenological, classical theory based essentially on the existence of elastic and inelastic MFP's. The main ingredients of the theory are the collisional processes inside the film and the reflections at the interfaces. The present formulation can be regarded as a generalization of conventional diffusion theory in the two-flux approximation[18,19] which allows for any finite number of well-defined energy-loss mechanisms, or, in a certain limit, as a continuous version of a one-dimensional random-walk theory.[20] The expression derived for the transmitted current depends on three unknown energy-dependent parameters. The elastic and the inelastic MFP's and the reflection coefficient at the film-metal interface. The fit of the experimental transmitted current as a function of the thickness and the energy determines the energy variation of these three parameters. The results are discussed in Sec. V.

II. EXPERIMENT

The apparatus consists of a high-resolution electron transmission spectrometer[21] of the type recently described in Sanche.[10] The spectrometer is housed in an ion- and titanium-pumped ultra-high-vacuum system reaching a base pressure of 5×10^{-11} Torr. The main components include a trochoidal monochromator, a pair of deflector plates, and a closed-cycle refrigerated cryostat of variable temperature (10—300 K). The magnetically collimated electrons leaving the monochromator are deflected by the plates and impinge on a film condensed on a metallic substrate attached to the cold end of the cryostat. The metal substrate (i.e., the electron collector) is electrically isolated from the cryostat by a sapphire sheet.

The trochoidal monochromator has been previously described in detail.[22] In the present experiment, the incident current $I_{\rm inc}$ is $\sim3\times10^{-9}$ A and the resolution 0.04 eV full width at half maximum (FWHM) as measured by retarding potential analysis in vacuum. Similar measurements on W(100) give a FWHM of 0.07 eV. As previously explained,[10] the use of deflector plates between the monochromator and the target can prevent, by the application of a suitable potential on these plates, any electrons reflected once from the target to reach it again. This configuration thus allows measurements of the absolute value of the transmitted current. Since the primary current intensity $I_{\rm inc}$ of magnetically confined electron beams is independent of energy at low current densities, the magnitude of the transmitted current becomes a quantitative determination of the overall transmission coefficient when $I_{\rm inc}$ is known. This latter can be measured by returning all scattered electrons to the metal substrate by retarding reflected electrons with the deflector plates.[10]

Experiments were performed on three different metal substrates: polycrystalline platinum and niobium sheets and a tungsten single-crystal disk (diameter 8 mm) with a surface oriented within 1° of the [100] direction. Before condensing the Xe film, the metallic substrate was either cleaned by resistive heating [1500 K for Pt and up to 2000 K for Nb and W(100)], or by argon sputtering followed by annealing at high temperatures. Both techniques gave the same transmission spectra. Matheson research-grade Xe gas was used (99.995% pure) without further purification. The gas was admitted in the vacuum system through a tube located in front of the collector. Most of the molecules (> 98%) leaving the tube condensed on the cryostat. The actual number which deposited on the collector was estimated from geometrical considerations and gas kinetic theory (i.e., expansion of a known volume of Xe at a given pressure and tem-

perature into vacuum),[7,10,23] assuming a sticking coefficient of unity. The number of monolayers condensed on the collector could be estimated by calibrating the amount of gas injected to produce "one" monolayer. The thickness of the film was then increased in steps of one monolayer using the calibrated values and assuming no change in sticking coefficients with film growth. The calibrated values were obtained by two different methods. The first approach consisted of measuring the change in work function corresponding to a unity coverage using the electron beam as previously described.[10] In the second method, the cryostat was held at 60 K. At this temperature only one monolayer of Xe can be condensed on the collector at 10^{-10} Torr. By monitoring the current on this latter while condensing the Xe, it was possible to measure the amount of injected gas required to observe no more change in the transmission spectrum. At this point we estimated that a monolayer of Xe had been formed. These combined measurements yielded an accuracy of 30% in estimated thicknesses with an average of 6 Å between layers. The error is systematic and only changes the scale of the values reported for MFP.

The temperature of the electron collector is maintained constant, controlled and monitored by a thermocouple (Au−0.07 at.% Fe versus Chromel copper) secured to the copper block of the cryostat. A difference of 2 K between the temperature of the copper block and that of the metal substrate was deduced from vapor pressure versus temperature data.[24]

For different thicknesses, the transmitted current was measured as a function of beam energy (0−20 eV). The sweep rate of the accelerating potential varied between 1 and 0.01 V/s. The energy scale was accurate within ±0.05 eV with respect to the injection curve. A number of tests previously described[25] was performed to ensure that the films did not change during each experiment.

III. RESULTS

Transmission spectra for different film thicknesses and temperatures (17 and 45 K) for Xe deposited on Nb,W(100) and Pt are shown in Figs. 1(a)−1(f). The temperature remained constant during the deposition and duration of the experiment. We clearly observe an energy displacement of the injection curve (zero energy) during the deposition of the first monolayer. This energy displacement is caused by the contact potential between the metal and covering Xe film. It is plotted in Fig. 2 for Nb and W(100) substrates as a function of coverage. For the Pt substrate we do not observe any perceptible change within our energy precision. The maximum displacement $|\Delta\phi|_{\max}$ is 0.55±0.05 eV for W(100) and 0.25±0.05 eV for Nb.

Some general observations should be made at this point.

(a) The transmission spectra pinpoint the onset of an inelastic region (~8 eV) exhibiting a maximum at 8.5 eV [first exciton energy of Xe (Refs. 14 and 16)]. The mechanism for producing a maximum at the exciton energy in the transmission spectra of molecular films has already explained.[25] It is summarized here and serves to explain the weak variation of the transmitted current with thickness in the energy region 8 eV $\lesssim E < 9.3$ eV (e.g., Fig. 3). This behavior is understood qualitatively[10,25]: at the onset of the inelastic process (~8 eV) an electron losing energy to create an exciton (8.5 eV) ends up at the bottom of the conduction band which lies 0.5 eV below the vacumm level.[13] It is no longer possible for this inelastically scattered electron to be backscattered into the vacuum (i.e., its energy lies below the vacuum level) and it contributes fully to the transmitted current. For high coverages the contribution of the elastic current becomes negligible and the transmitted current becomes independent of the thickness. As the incident energy increases, the number of energy-loss electrons increases until their energies reach the vacuum level. Above this incident energy (8.5 eV), inelastic electrons can be backscattered into vacuum and the transmitted current, which is almost purely inelastic for large thicknesses [see Eq. (4) in the next section], can decrease. A maximum in the transmitted current can therefore be expected at 8.5 eV for large thicknesses.

(b) If the incident energy is increased beyond 8.8 eV, the electron energy inside the film is equal to 8.8+0.5=9.3 eV, the energy gap of xenon.[14] At this energy, the colliding electrons may excite a valence electron into the conduction band. For incident energies above 8.8+0.5=9.3 eV (the photoemission threshold[8] is 9.8 eV =9.3+0.5), the final energy of one of the two electrons in the conduction band is above vacuum and it may eventually be backscattered into vacuum, thus decreasing the transmitted current. A maximum is thus expected at 9.3 eV. Above this energy, the transmitted current decreases and can change sign (hole current) if the secondary emission coefficient becomes greater than unity.

(c) As shown in the next section the 1−8 eV region can be described in terms of a purely elastic

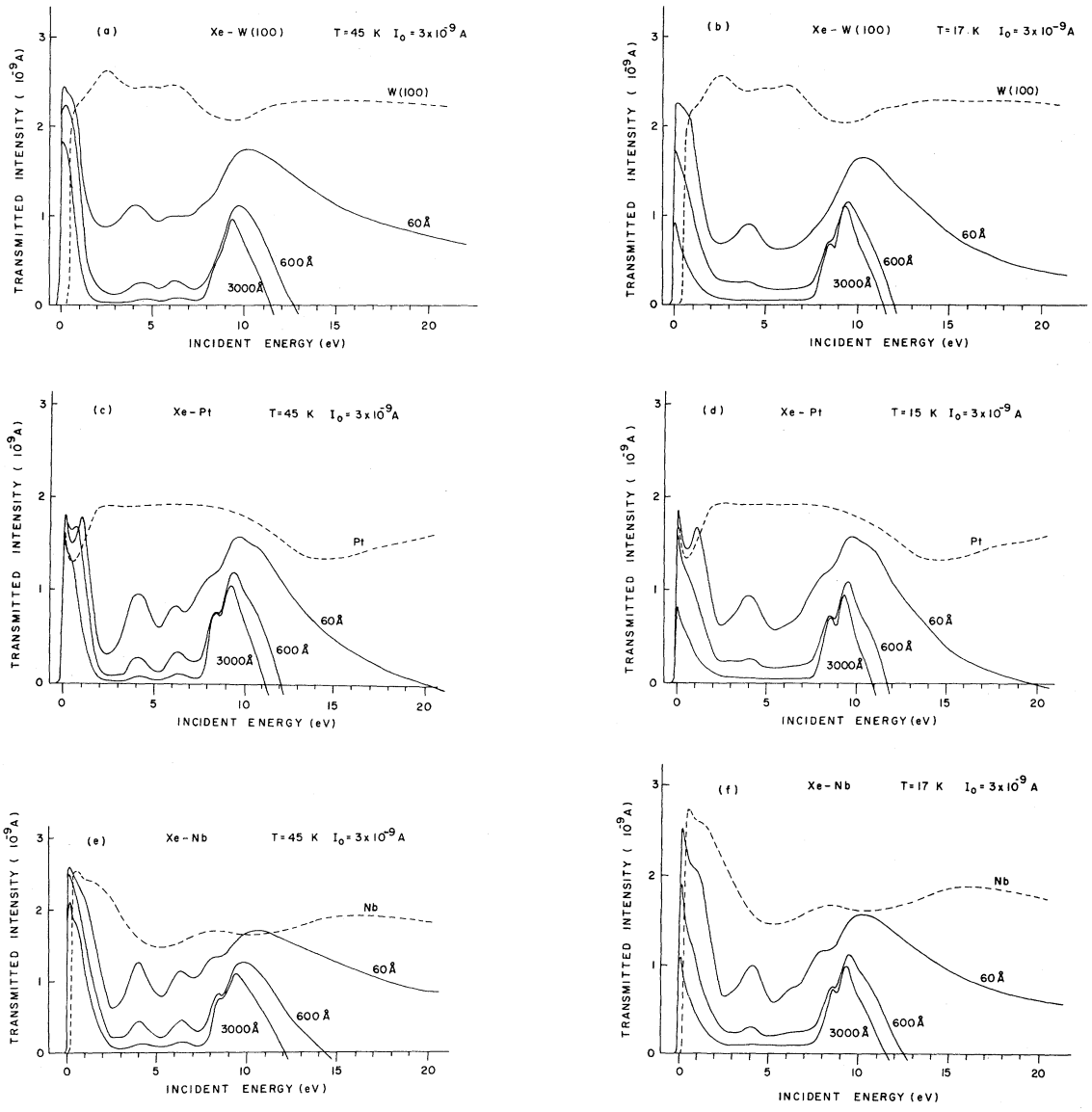

FIG. 1. Transmitted current vs electron energy in Xe films deposited on three different substrates at 17 and 45 K. The thickness of the film is indicated at the right of each curve.

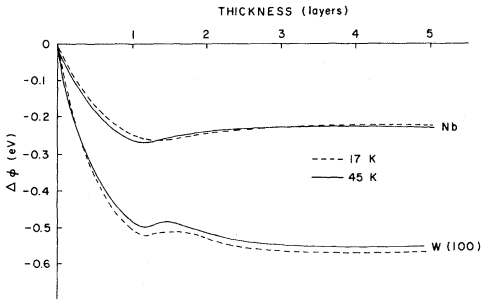

FIG. 2. Change in the substrate work function $\Delta\phi$ as a function of thickness for Xe on W(100) and Nb at 17 and 45 K.

scattering process. The amplitude of the structures in this region varies with the deposition temperature. Figure 4 shows spectra for films deposited at 17 and 45 K on Pt, and others deposited at 45 K and then cooled to 17 K. The three curves are very different. The films deposited at 17 K are presumably the most disordered ones (structural disorder). In the films deposited at 45 K, the structural disorder is smaller but there is greater thermal disorder (phonons) than in the 17-K deposited films. The films deposited at 45 K and cooled to 17 K are likely the most ordered ones: low structural disorder because of the high deposition temperature and low

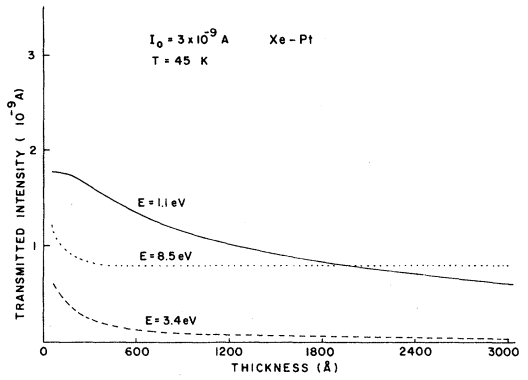

FIG. 3. Thickness dependence of transmitted current at 1.1, 3.4, and 8.5 eV for a 45-K deposition on Pt.

thermal disorder, since at 17 K the phonon population is well reduced (Debye temperature: 64 K).[26] The structures between 1 and 8 eV are apparently closely related to the ordering of the films which are surely not purely monocrystalline. Further experiments on 17-K deposited films, and heated to different temperatures and then cooled, show the existence of a structural reordering. Furthermore, the cooling of an ordered film gives the telltale signs of thermal disorder (Debye-Waller factor). These aspects shall be quantitatively analyzed in a separate publication.

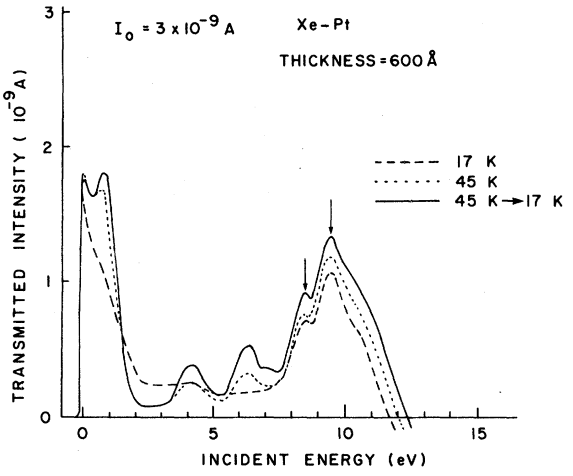

FIG. 4. Transmission spectra for Xe films deposited at 45 K ($\cdots$), 17 K ($- - -$), and 45 K but cooled to 17 K (——) on Pt. The thickness was 600 Å. The vertical arrows indicate the energy of the most intense excitonic transitions.

IV. THEORY

In this section, a classical theoretical model is developed in order to obtain useful quantitative information from the experimental data. The scattering phenomena inside the film are taken into account by means of elastic and inelastic MFP's. We have neglected the collisional processes between conduction electrons as well as the inelastic losses due to phonons. Indeed, the small values of the incident current (3×10^{-9} A), the average time an electron resides inside the film ($10^{-12}-10^{-11}$ s), and the small electron-phonon coupling constant[8] indicate that these interactions can be neglected.

During their stay within the film, electrons are assumed to have energy-dependent probabilities per unit length of undergoing an elastic or an inelastic collision. The inverse of these probabilities define the elastic and inelastic mean free paths. Hereon, we follow the work of a number of authors,[19,27,28] particularly Chantry *et al.*[19] and we write the following set of equations in the two-stream approximation with isotropic scattering and the stationary limit:

$$\frac{dS^+_{E_0}}{dx} = -\left[\frac{1}{l_e(E_0)}+\frac{1}{l_i(E_0)}\right]S^+_{E_0}\,,$$

$$\frac{dS^-_{E_0}}{dx} = \left[\frac{1}{l_e(E_0)}+\frac{1}{l_i(E_0)}\right]S^-_{E_0}\,, \tag{1a}$$

$$\frac{dI^+_{E_0}}{dx} = -\epsilon\left[\frac{1}{2l_e(E_0)}+\frac{1}{l_i(E_0)}\right]I^+_{E_0} + \frac{\epsilon}{2l_e(E_0)}I^-_{E_0}+\frac{1}{2l_e(E_0)}(S^+_{E_0}+S^-_{E_0})\,,$$

$$\frac{dI^-_{E_0}}{dx} = -\frac{\epsilon}{2l_e(E_0)}I^+_{E_0} + \epsilon\left[\frac{1}{2l_e(E_0)}+\frac{1}{l_i(E_0)}\right]I^-_{E_0} - \frac{1}{2l_e(E_0)}(S^+_{E_0}+S^-_{E_0})\,,$$

where $1/l_e$, $1/l_i$, and E_0 are the probability per unit length for an electron to be elastically, inelastically scattered, and the incident energy, respectively. $S^+_{E_0}$,$S^-_{E_0}$ are the current densities for an unscattered electron of energy E_0 at a depth x in the forward or backward direction, respectively. The x axis is perpendicular to the film $x=0$ gives the position of the vacuum-film interface, and $x=L$ that of the film-metal interface. Note that $S^-_{E_0}$ is nonzero due to the possible specular reflection at the film-metal interface. $I^+_{E_0}$ and $I^-_{E_0}$ are the current densities for already elastically scattered electrons of energy E_0 at a depth x in the forward or backward direction, respectively. The parameter ϵ is related to the angular distribution of electrons and varies usually between 1 and 2. The equations are essentially the same as those in Ref. 19 with some change in the definition of the parameters. We wish to point out that a similar set of equations (with $\epsilon=1$ and $l_i\rightarrow\infty$) can be obtained from a continuum version of a one-dimensional random-walk theory which has already been used to study the distribution of defects in solids.[20] The inelastic currents are introduced in the same way as in Eq. (1a). We considered only one inelastic well-defined energy loss, but this can be easily generalized to any finite number of inelastic well-defined losses. Two more equations complete the set of Eq. (1a):

$$\begin{aligned}\frac{dJ^+_{E'}}{dx}=&-\frac{\epsilon}{2l_e(E')}J^+_{E'}+\frac{\epsilon}{2l_e(E')}J^-_{E'}\\&+\frac{\epsilon}{2l_i(E_0)}(I^+_{E_0}+I^-_{E_0})\\&+\frac{1}{2l_i(E_0)}(S^+_{E_0}+S^-_{E_0}),\\ \frac{dJ^-_{E'}}{dx}=&-\frac{\epsilon}{2l_e(E')}J^+_{E'}+\frac{\epsilon}{2l_e(E')}J^-_{E'}\\&-\frac{\epsilon}{2l_i(E_0)}(I^+_{E_0}+I^-_{E_0})\\&-\frac{1}{2l_i(E_0)}(S^+_{E_0}+S^-_{E_0}),\end{aligned}\tag{1b}$$

where $J^+_{E'}$ and $J^-_{E'}$ are the current densities for inelastically scattered electrons of final energy E' at a depth x in the forward or backward direction respectively. We have used here the same parameter ϵ as for the elastically scattered currents. Let us consider the boundary conditions. They must involve all the reflections at the two interfaces. Since $I^\pm$,$J^\pm$ describe already scattered electrons, their reflection must be considered as diffuse. On the contrary, $S^\pm$ includes unscattered electrons and the reflection for such electrons may be specular or diffuse depending on the quality of the interfaces. If the interfaces are not well defined or not perfect, the reflected electrons of $S^\pm$ must then be considered as scattered. We write the boundary conditions in the following way:

$$\begin{aligned}&S^+_{E_0}(0)=\alpha R_S(E_0)S^-_{E_0}(0)+I_0,\\&S^-_{E_0}(L)=\alpha' R'_s(E_0)S^+_{E_0}(L),\\&I^+_{E_0}(0)=R(E_0)I^-_{E_0}(0)+(1-\alpha)R(E_0)S^-_{E_0}(0),\\&I^-_{E_0}(L)=R'(E_0)I^+_{E_0}(L)\\&\qquad+(1-\alpha')R'(E_0)S^+_{E_0}(L),\\&J^+_{E'}(0)=R(E')J^-_{E'}(0),\\&J^-_{E'}(L)=R'(E')J^+_{E'}(L),\end{aligned}\tag{2}$$

where R_S and R'_S (R,R') are the specular (diffuse) reflection coefficients at the vacuum-film and film-metal interfaces, respectively. The parameters α,α' characterize the state of the two interfaces and vary between 0 and 1. The transmitted current can then be written as

$$\begin{aligned}I_{\text{trans}}=&S^+_{E_0}(L)-S^-_{E_0}(L)+I^+_{E_0}(L)-I^-_{E_0}(L)\\&+J^+_{E'}(L)-J^-_{E'}(L).\end{aligned}\tag{3}$$

The solution is now a matter of mathematics. As we have restricted our analysis for Xe to the (0—8.5)-eV energy range, the electrons can undergo at most one inelastic collision and their final energies will be below the vacuum level. This implies that the inelastic electrons cannot return in the vacuum and, thus, that $R(E')=1$. We give below the transmitted current in this case,

$$A_0=\frac{I_0}{1-\alpha\alpha' R_s R_s' e^{-2\sigma_T L}},\quad B_0=\alpha' R_s' A_0 ,$$

$$\sigma_i=\frac{1}{l_i},\quad \sigma_T=\frac{1}{l_e}+\frac{1}{l_i},\quad m=\frac{\sigma_i}{\sigma_T},\quad y=\epsilon m^{1/2} ,$$

$$\rho=\epsilon\frac{1-R}{1+R},\quad \rho'=\epsilon\frac{1-R'}{1+R'} ,$$

$$Z=\rho'\cosh(y\sigma_T L)+y\sinh(y\sigma_T L) ,$$

$$D=(\rho+\rho')\cosh(y\sigma_T L)+\frac{\rho\rho'}{y}\sinh(y\sigma_T L)+y\sinh(y\sigma_T L) , \tag{4}$$

$$N=A_0[\rho(1-\rho')e^{-\sigma_T L}+(1+\rho)Z]-B_0[\rho(1+\rho')e^{-\sigma_T L}+(1-\rho)e^{-2\sigma_T L}Z] ,$$

$$I_{\text{trans}}=\frac{\epsilon^2-y^2}{1-y^2}\frac{1}{\epsilon^2}\frac{N}{D}+\frac{1-\epsilon^2}{1-y^2}\frac{y^2}{\epsilon^2}(A_0-B_0e^{-2\sigma_T L})+B_0(1-\alpha)\left[1-\frac{\rho}{\epsilon}\right]\frac{Z}{D}e^{-2\sigma_T L}$$
$$-A_0(1-\alpha')\left[1-\frac{\rho'}{\epsilon}\right]\frac{\rho}{D}e^{-\sigma_T L} .$$

Note that there is no divergence when $y=1$.

We give below some useful limits for the transmitted current.

(i) If $\alpha'=0$, then

$$I_{\text{trans}}(L=0)=I_0\frac{1-R'}{1-RR'} .$$

(ii) If $\alpha'=1$, $\alpha=1$, then

$$I_{\text{trans}}(L=0)=I_0\frac{1-R_s'}{1-R_sR_s'} .$$

(iii) If $y=0$ ($l_i\to\infty$), $R_s'=0$, $\alpha'=1$, we find the same results as Chantry *et al.*[19]:

$$I_{\text{trans}}(L)=I_0\frac{\rho'(\rho+1)-\rho(\rho'-1)e^{-\sigma_e L}}{\rho+\rho'+\rho\rho'\sigma_e L} .$$

(iv) If $y=\epsilon$ ($l_i\to 0$), then $I_{\text{trans}}(L)=I_0$.

(v) If $y\neq 0$ ($l_i\neq\infty$), then $\lim_{L\to\infty} I_{\text{trans}}(L)=C(y)$ with $C(y)$ an increasing function of y with $C(0)=0$ and $C(\epsilon)=I_0$. This means that the transmitted current becomes almost thickness independent for large thickness and that the value of the current increases from zero to I_0 if l_i decreases from infinity to zero.

We fitted the experimental curves with the above model in order to determine, among other things, the energy variation of the mean free paths. It was useful, if not essential, to decrease the number of known parameters. Since no special measures were taken to control the state of each interface, we assumed that they were imperfect and that the reflection was nonspecular, i.e., $\alpha=\alpha'=0$. Furthermore, we represented the potential at the vacuum-film interface by a step barrier V. The energy dependence of R was then automatically determined[29] as

$$R(E)=\left[\frac{V}{V+E}\right]^{1/2} . \tag{5}$$

Since the bottom of the first conduction band is at 0.5 eV below vacuum,[13] we took $V=0.5$ eV. The parameter ϵ was set equal to one. Note that V and ϵ were varied in a second stage of the fit in order to justify our choice. During this verification, the best fit gave $V=0.47$ eV and $\epsilon=1.1$ for 45-K deposited films. I_0 has theoretically the value TI_{inc} where I_{inc} is the incident current density and T the quantum-mechanical transmission factor through the vaccum-film interface. Since this interface was modeled by a weak potential barrier, we took $T=1$. The parameters l_e, l_i, R' were obtained by fitting the transmitted current versus thickness curves at anywhere between 18 and 36 different energy values depending on the film and on the precision needed. For 500 points (18 energy values), we had $\sum_{i=1}^{500}(\text{experiment}-\text{theory})^2<\sim 10^{-19}$ A^2. The mean error was thus of the order of the experiment uncertainty (2×10^{-11} A) on the electron current. Figures 5(a)–5(c) show the energy dependence of the elastic MFP obtained for Xe films deposited at 17 K and 45 K on Nb, W(100), and Pt, respectively. In Fig. 5(c), we have added the spectrum for a film deposited at 45 K on platinum but recorded at 17 K. We recall that the major error source on these results comes from the uncertainty (30%) in the

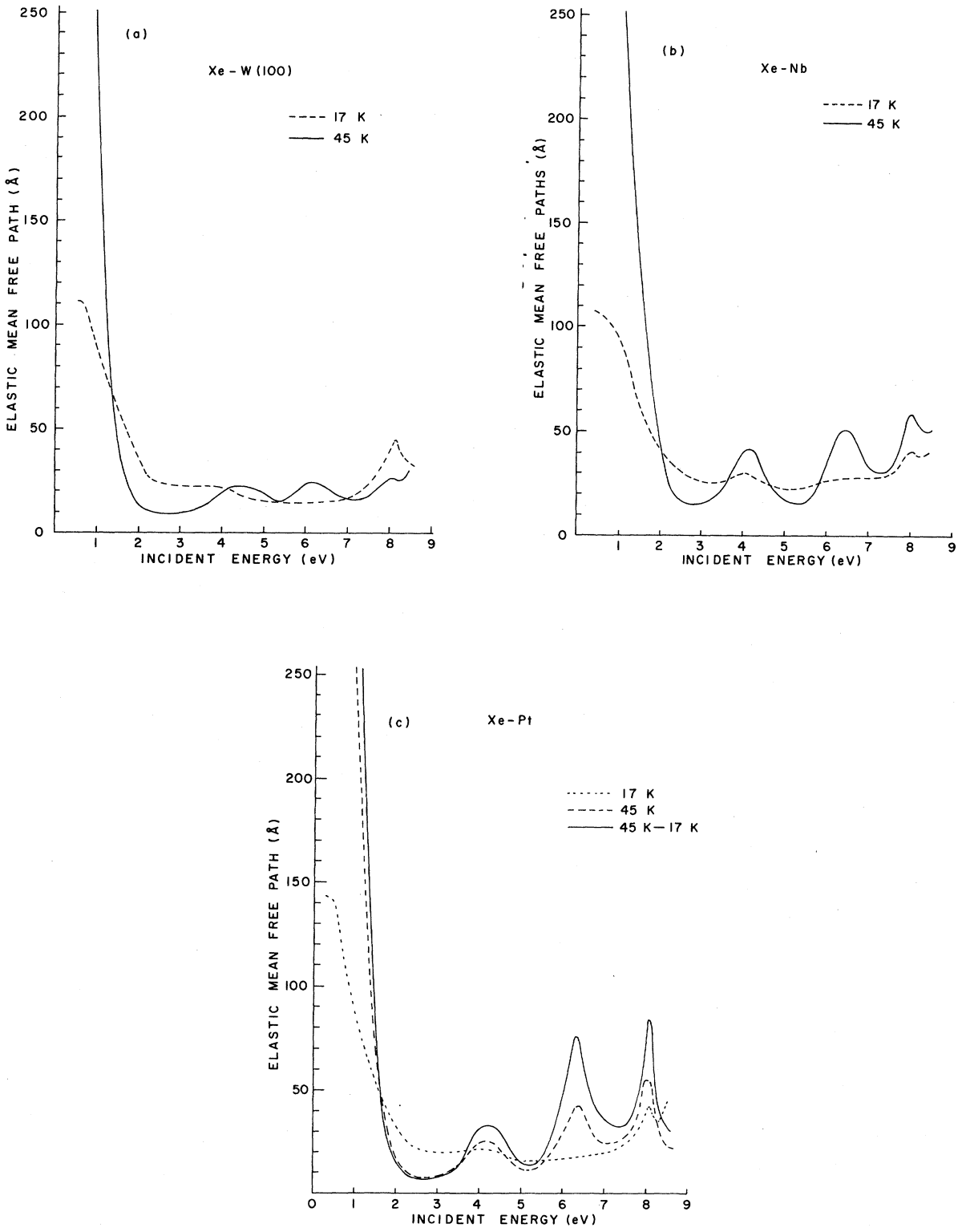

FIG. 5. Elastic mean free paths (MFP's) plotted as a function of incident energy for Xe films on Nb and W(100) deposited at 17 and 45 K. Figure 5(c) includes also the MFP for a 45-K deposited film cooled to 17 K on Pt.

determination of the length scale although it is probably possible to determine by more accurate methods the absolute thickness of the films. Figure 6 shows a typical energy dependence of the inverse of the inelastic MFP for a 17-K deposited film and also for a 45-K deposited film which was cooled to 17 K. The value of R' are such that $I_0[(1-R')/1-RR')]$ follows roughly the behavior of an experimental $I_{\text{trans}}(E)$ curve at a thickness of the order of 10–20 Å on the given metal.

V. DISCUSSION

Before discussing the results presented in Figs. 5 and 6, it is important to fully understand some of the constraints injected into our theoretical model. The choice $\alpha=\alpha'=0$ eliminates all specular reflections. This is certainly reasonable at high energies (or short wavelengths) when the electrons are sensitive to the imperfections in the interfaces. But this is no longer correct when the wavelength of the low-energy electron is large enough that it "sees" smoothed interfaces. Thus, specular reflections must become important at low energies. This is quite flagrant when the MFP is larger than the thickness of the film and multiple interferences set in. As a matter of fact, we did observe poorer fits for low energies (<1 eV) and small thicknesses (<100 Å). Furthermore, it can be verified using Eq. (4) that the transmitted current versus thickness can have a maximum (as observed in Fig. 3) only if α and α' are nonzero.

The representation of the film-vaccum interface by a potential barrier [Eq. (5)] is also a crude approximation. Such a modelization does not take into account any change in the effective mass of the electron inside the film.

An important feature observed in Fig. 5 is the rapid increase of the MFP with decreasing energy below 2 eV. Although straightforward wavelength arguments imply such an increase (at large wavelength, the electrons "see" the film as a continuum), there is one additional contribution which must also be considered. The behavior of the MFP must obviously be related in some way to the energy dependence of the total scattering cross section σ_g of atomic Xe measured in the gas phase.[30] This cross section is presented in Fig. 7 and compared to the effective cross section σ_S obtained from the MFP though a density factor (fcc, $a=6.17$ Å) for a 17-K deposited film on Pt. Note that the zero of energy for σ_S is at the bottom of the conduction band. In the frozen gas limit (independent atomic t matrices), these cross sections are theoretically related through a well-known relation[31]

$$\frac{d\sigma_S}{d\Omega}=\frac{d\sigma_g}{d\Omega}S(kk') , \tag{6}$$

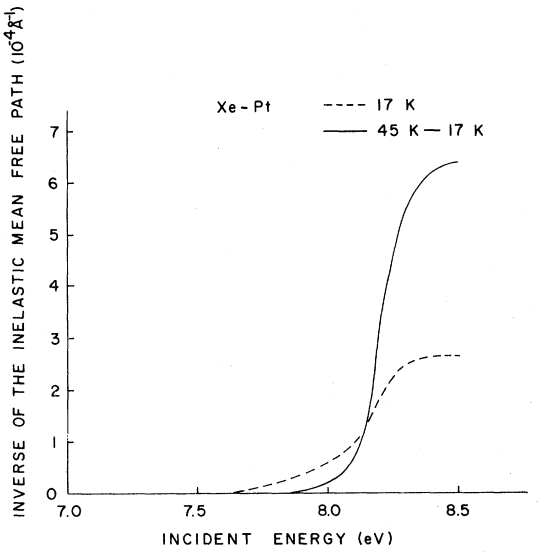

FIG. 6. Energy dependence of the inverse of the inelastic MFP for a 17-K deposited film and a 45-K deposited film cooled to 17 K on Pt.

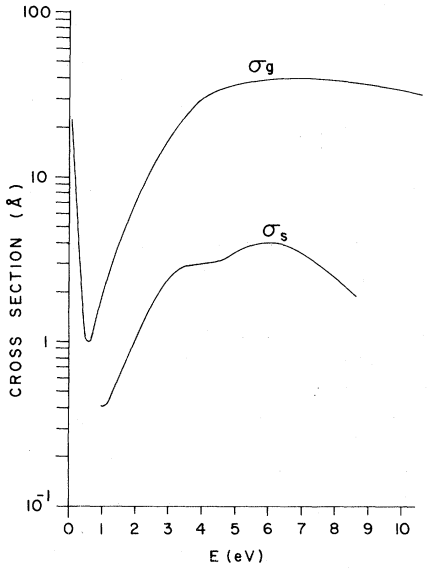

FIG. 7. Energy dependence of total electron scattering cross section in Xe gas (σ_g) (see Ref. 30) and in solid Xe (σ_S) for a 17-K deposition on Pt. The zero energy in the solid is taken as the bottom of the conduction band.

where $d\sigma_S/d\Omega$, $d\sigma_g/d\Omega$, and S are the differential cross sections for the "frozen gas" solid, the gas, and the structure factor of the material, respectively. The above relation indicates that the rapid increase of the MFP below 2 eV is due to the Ramsauer minimum in σ_g or/and to a sharp decrease in the structure factor. This equation also gives a clue as to the origin of the structures observed in the transmitted current at energies between 1 and 8 eV. In our fit, these structures could be directly correlated with the elastic MFP but not the inelastic one [see Figs. 5(c) and 6]. They were also clearly related to the structural and thermal order in the film. An energy and atomic order dependence of the structure factor can possibly explain these phenomena qualitatively. Indeed, we note that the first Bragg reflection, which is estimated to occur at 2.99 eV above the bottom of the conduction band for the fcc structure of Xe ($a=6.17$ Å), does correlate with the first minimum in the MFP's of well-ordered films. An analysis of the correlation between Bragg peaks and transmission minima will be presented in a separate publication.

As far as the inelastic processes are concerned, Fig. 6 is highly instructive. We observe that the energy difference between the bottom of the conduction band and the vacuum (0.5 eV) is clearly related to the difference between the onset of the inelastic exciton creation and the exciton energy in the more ordered films. Furthermore, the curve relating to what we believe to be the disordered film reveals a less well-defined onset of the inelastic process. This is perhaps due to a smearing of the states near the bottom of the conduction band. The probability of exciton creation is apparently decreased by the disorder.

In summary, we have shown how to extract some quantitative information from low-energy electron transmission experiments. Within a scale factor uncertainty of 30%, we have determined the absolute values for the MFP's and indicated that they are very sensitive to structural and thermal disorder. In forthcoming theoretical and experimental work, more precise information is extracted from such data.

ACKNOWLEDGMENTS

We would like to thank Marc Michaud for the numerous and fruitful discussions we had on these experiments. The work of G. B. and L. G. was sponsored by the Natural Sciences and Engineering Research Council of Canada. The work of G. P. and L. S. was sponsored by the Medical Research Council of Canada.

*Present address: Département de Physique et Mathématiques, Université de Moncton, Moncton, N. B. E1A 3E9, Canada.

[1]W. E. Spicer, J. Phys. Chem. 22, 365 (1961).
[2]G. W. Gobeli and F. G. Allen, Phys. Rev. 127, 141 (1962).
[3]J. L. Shay and W. E. Spicer, Phys. Rev. 169, 650 (1968).
[4]S. W. Duckett and P. H. Metzger, Phys. Rev. 137, A953 (1965).
[5]W. Pong, J. Appl. Phys. 37, 3033 (1966).
[6]A. D. Baer and G. J. Lapyere, Phys. Rev. Lett. 31, 304 (1973).
[7]Y. C. Chang and W. B. Berry, J. Chem. Phys. 61, 2727 (1974).
[8]N. Schwentner, Phys. Rev. B 14, 5490 (1976).
[9]S. Hino, N. Sato, and H. Inokuchi, J. Chem. Phys. 67, 4139 (1977).
[10]L. Sanche, J. Chem. Phys. 71, 4860 (1979).
[11]D. Menzel, in *Photoemission and the Electronic Properties of Surfaces,* edited by B. Fenerbacher, B. Fitton, and R. F. Willis (Wiley-Interscience, New York, 1978).
[12]J. B. Pendry, *Low Energy Electron Diffraction* (Academic, New York, 1974).
[13]N. Schwentner, F.-J. Himpsel, V. Saile, M. Skibowski, W. Steinmann, and E. E. Koch, Phys. Rev. Lett. 34, 528 (1975).
[14]R. Haensel, G. Keitel, E. E. Kock, N. Kosuch, and M. Skibowski, Phys. Rev. Lett. 25, 1281 (1970).
[15]A. Ignatiev, A. V. Jones, and T. N. Rhodin, Surf. Sci. 30, 573 (1972).
[16]H. H. Farrell and M. Strongin, Phys. Rev. B 6, 4711 (1972).
[17]M. L. Klein and T. R. Koehler, in *Lattice Dynamics of Rare Gas Solids,* edited by M. L. Klein and J. A. Venables (Academic, New York, 1976).
[18]S. Chandrasekhar, *Radiative Transfer* (Clarendon, Oxford, 1950).
[19]P. J. Chantry, A. V. Phelps, and G. J. Schulz, Phys. Rev. 152, 81 (1966).
[20]P. Grassberger, Physica (Utrecht) 103A, 558 (1980).
[21]L. Sanche and G. J. Schulz, Phys. Rev. A 5, 1672 (1972).
[22]A. Stamatovic and G. J. Schulz, Rev. Sci. Instrum. 41, 423 (1970).
[23]T. E. Madey, Surf. Sci. 33, 355 (1972).
[24]R. E. Honing and H. O. Hook, R. C. A. Rev. 21, 360

(1960).
[25]L. Sanche, G. Bader, and L. Caron, J. Chem. Phys. 76, 4016 (1982).
[26]Charles Kittel, *Introduction to Solid State Physics,* 4th ed. (Wiley, New York, 1971).
[27]J. P. McKelvry, R. L. Longini, and T. P. Brody, Phys. Rev. 123, 51 (1961).
[28]W. Shockley, Phys. Rev. 125, 1570 (1962).
[29]P. A. Wolff, Phys. Rev. 95, 56 (1954).
[30]L. S. Frost and A. V. Phelps, Phys. Rev. 136, A1538 (1964).
[31]J. M. Ziman, *Principles of the Theory of Solids,* 2nd ed. (Cambridge University Press, Cambridge, England, 1972).